

ANALYTIC METHODS OF SIMULATING MAGNETIC FIELDS FOR THE TAIWAN PHOTON SOURCE

C. Y. Kuo[#], C.S. Hwang, F. Y. Lin and C. H. Chang, NSRRC, HsinChu, Taiwan

Abstract

Analytic methods of four kinds served for analysis of the magnetic field of TPS magnets that were simulated with OPERA 2D and 3D software. These analytic methods include fast Fourier transform, one-dimensional fitting, two-dimensional circular or elliptic fitting and a differential field. In this paper we discuss the precision of varied analytic methods for properties of a magnetic field in various situations.

INTRODUCTION

The accelerator magnets for Taiwan Photon Source (TPS) were manufactured and measured in the past three years. For various magnets, several methods of measurement and analytic methods were utilized to derive the multipole components. In experiments, quadrupole and sextupole magnets were measured with a rotating-coil system and analyzed with a fast Fourier transform.[1] The multipole components of bending magnets with a large pole gap were measured with a Hall probe system and analyzed with a two-dimensional elliptic fitting method. The multipole components of bending magnets with a small pole gap were measured with a Hall probe system and analyzed with one-dimensional fitting and a differential-field method. In this paper we introduce these four analytic methods and compare the analytic results of ideal cases simulated with OPERA 2D and 3D software.

ANALYTIC METHODS

The magnetic field $B_x + iB_y$ is expressed in polynomial expansions as

$$B_x + iB_y = \sum (a_n + ib_n)(x + iy)^n \quad (1)$$

in which a_n and b_n denote the skew and normal components respectively.

When

$n=0$, the right side of the equation equals $\text{Re}[a_0] + \text{Im}[b_0]$,
 $n=1$, $\text{Re}[a_1x - b_1y] + \text{Im}[a_1y + b_1x]$,
 $n=2$, $\text{Re}[a_2x^2 - a_2y^2 - 2b_2xy] + \text{Im}[2a_2xy + b_2x^2 - b_2y^2]$
 and so on; the equation is then divided into real part B_x and imaginary part B_y .

$$B_y(x, y) = b_0 + a_1y + b_1x + 2a_2xy + b_2(x^2 - y^2) + \dots \quad (2)$$

$$B_x(x, y) = a_0 + a_1x - b_1y - 2b_2xy + a_2(x^2 - y^2) + \dots \quad (3)$$

One-dimensional fitting method

As a Hall-probe system typically measures the normal field B_y along the transverse axis for a dipole magnet, only $B_y(x)$ is discussed in this paper.

$$B_y(x, 0) = b_0 + b_1x + b_2x^2 + \dots \quad (4)$$

Fitting a polynomial with a large number as order could have a large effect on multipole components from a data source of little accuracy. This discussion is presented with the results of simulation with OPERA software.

Two-dimensional fitting method

A two-dimensional fitting equation applies Eq. 2 or 3. The positions of two-dimensional field data are measured as circular or elliptic. Circular data can be superior to elliptic data; the order of fitting does not affect the multipole components of circular data, but components of high order could have large errors from elliptic data. In real experimental conditions, a dipole magnet could be measured to derive elliptic data but not circular data because of limited space in the gap of the magnet. A comparison of circular and elliptic data is discussed below.

Fast Fourier-transform method

OPERA 2D documentation [2] shows the fast Fourier fitting divided into two parts:

even function $F(s)=F(-s)$

odd function $F(s)=-F(-s)$

skew terms $a_0=0$

$$a_n = \sum_{m=1}^P \left[\frac{2S_m}{2\pi n} \int_0^{1/P} \sin(2\pi ns) F(s) ds \right] \quad (5)$$

$$b_0 = \sum_{m=1}^P \left[\frac{S_m}{2\pi} \int_0^{1/P} F(s) ds \right] \quad (6)$$

$$b_n = \sum_{m=1}^P \left[\frac{2S_m}{2\pi n} \int_0^{1/P} \cos(2\pi ns) F(s) ds \right] \quad (7)$$

s : normalized measure of distance along the line,

$F(s)$: component that is being fitted,

P : value of the period parameter, and

S_m : sign function equal to +1 or -1.

For example, when Period=4,

series=even: this condition implies $S_1=1 S_2=-1 S_3=-1 S_4=1$

series=odd: this condition implies $S_1=1 S_2=1 S_3=-1 S_4=-1$

Differential-field method

$$B_y(x) = b_0 + b_1x + b_2x^2 + \dots \quad (8)$$

$$\frac{dB_y}{dx} = B'_y(x) = b_1 + b_2 x + b_3 x^2 + \dots \quad (9)$$

$$\frac{d^2B_y}{dx^2} = B''_y(x) = b_2 + b_3 x + b_4 x^2 + \dots \quad (10)$$

$$B_y(0) = b_0 \quad (11)$$

$$B'_y(0) = b_1 \quad (12)$$

$$B''_y(0) = b_2 \quad (13)$$

OPERA 2D RESULTS

The pole gap of the TPS dipole magnet in the storage ring is 24 mm. The range of measurement is between -20 mm and +20 mm along the x axis for one-dimensional fitting and the differential method. The radius of measurement is 20 mm for two-dimensional circular fitting and the fast Fourier-transform method. Normal field components of dipole magnet are discussed; skew field components of dipole magnet are ignored because the skew term values are too small. The normalized value of a normal multiple component is discussed to compare the difference of these four analytic methods as table 1 shows. The normalization of the dipole field is defined as $(b_n/b_0)x^n$ or $(b_n/b_0)r^n$. OPERA 2D results show satisfactory consistency of separate methods. The difference of these four methods is within 1 ppm at allowed terms Nb_2 , Nb_4 , Nb_6 and Nb_8 . In one-dimensional fitting analysis, the fitting number should be between 11 and 25 according to a Nb_8 variation of a fit number as in Fig. 1. Figure 2 shows the differential field method; the curve of the eighth differential distribution of $B_y(x)$ is smooth, which implies satisfactory continuity data of the magnetic field.

Table 1: Results of a dipole magnet simulated with OPERA 2D for analytic methods of four kinds

| <i>n</i> | 1D (fn8) | 1D (fn16) | 2D CIR. (fn8) | FFT | DIFF. |
|-----------------|---------------------|----------------------|------------------------------|------------|--------------|
| 0 | 10000 | 10000 | 10000 | 10000 | 10000 |
| 1 | -0.001 | -0.001 | -0.001 | -0.003 | -0.001 |
| 2 | 0.089 | 0.088 | 0.088 | 0.088 | 0.089 |
| 3 | -0.001 | -0.001 | -0.001 | 0.002 | -0.001 |
| 4 | 0.100 | 0.110 | 0.110 | 0.109 | 0.108 |
| 5 | 0.001 | 0.000 | 0.000 | -0.002 | 0.000 |
| 6 | 0.003 | -0.024 | -0.024 | -0.023 | -0.028 |
| 7 | 0.000 | 0.001 | 0.001 | 0.002 | 0.001 |
| 8 | -0.057 | -0.028 | -0.029 | -0.031 | -0.035 |

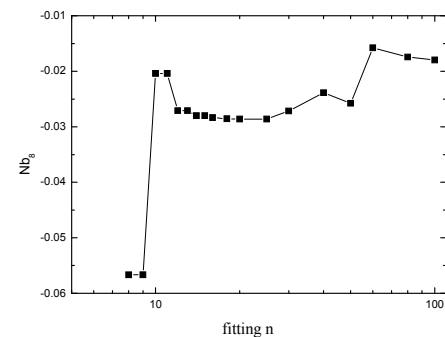


Figure 1: Variation of fitting number of Nb_8 .

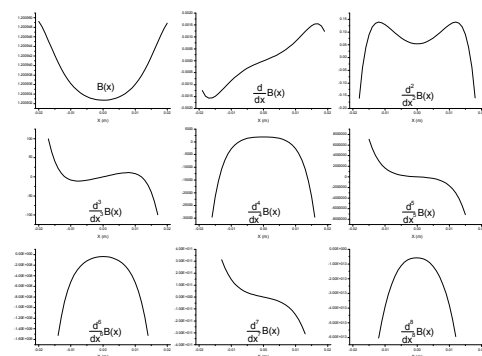


Figure 2: Eighth differential of $B_y(x)$ in OPERA 2D.

Measuring an elliptic long axis $R_a = 20$ mm and a short axis $R_b = 10$ mm with the two-dimensional elliptic fitting is shown in table 2. The fit number of elliptic fitting affects the multipole components of high orders; there is 3 ppm deviation of Nb_8 , and the result of fit number 13 is similar to the circular fit result. Multipole components of high order thus have poor accuracy in 2D elliptic fitting.

Table 2: Results of varied fit number of two-dimensional elliptic fits

| <i>n</i> | 2D ELL. (fn8) | 2D ELL. (fn13) | 2D ELL. (fn20) |
|-----------------|--------------------------|---------------------------|---------------------------|
| 0 | 10000 | 10000 | 10000 |
| 1 | -0.001 | -0.001 | -0.001 |
| 2 | 0.089 | 0.088 | 0.088 |
| 3 | -0.001 | -0.001 | -0.001 |
| 4 | 0.106 | 0.110 | 0.110 |
| 5 | 0.001 | 0.000 | 0.000 |
| 6 | -0.009 | -0.024 | -0.025 |
| 7 | 0.000 | 0.001 | 0.001 |
| 8 | -0.048 | -0.027 | -0.023 |

OPERA 3D RESULTS

An OPERA 2D dipole-magnet model was inserted into OPERA 3D and its length extended. Ideally, the central fields of OPERA 2D and OPERA 3D should be the same, but it was difficult to have the mesh size of OPERA 3D the same as with 2D. Here follow two cases: one is a fine

mesh size of which the mesh point to point is 1 mm; the other is a coarse mesh size with mesh point to point 5 mm.

Table 3 lists four analytic results of a fine-mesh OPERA 3D model; the 2D circle fitting result is nearly the same as the fast Fourier-transform result and also near the OPERA 2D results. The difference of 2D fits between OPERA 2D and 3D is within 1 ppm at allowed term Nb_2 , but there was a large difference between 1D fits and the differential method from OPERA 2D. The difference of Nb_8 in differential methods of OPERA 2D and OPERA 3D was four parts in ten thousand. Results of 1D fits show that fit number 8 is nearer 2D fitting and FFT than number 16. The fit number for 1D fits has thus a larger effect in OPERA 3D than in OPERA 2D. Table 4 lists the field results of a OPERA 3D model. with a coarse mesh

Table 3: OPERA 3D dipole magnet with a fine mesh

| <i>n</i> | 1D (fn8) | 1D (fn16) | 2D CIR. (fn8) | FFT | DIFF. |
|-----------------|--------------------|---------------------|----------------------------|------------|--------------|
| 0 | 10000 | 10000 | 10000 | 10000 | 10000 |
| 1 | -0.002 | -0.002 | -0.002 | -0.002 | -0.002 |
| 2 | 0.079 | 0.078 | 0.075 | 0.075 | 0.076 |
| 3 | -0.004 | -0.004 | -0.004 | -0.003 | -0.004 |
| 4 | 0.098 | 0.085 | 0.107 | 0.107 | 0.181 |
| 5 | -0.002 | -0.003 | -0.002 | -0.002 | -0.002 |
| 6 | 0.008 | 0.189 | -0.021 | -0.021 | -0.820 |
| 7 | 0.000 | 0.009 | 0.000 | 0.000 | 0.002 |
| 8 | -0.058 | -0.918 | -0.027 | -0.027 | 4.702 |

Table 4: OPERA 3D dipole magnet with a coarse mesh

| <i>n</i> | 1D (fn8) | 1D (fn16) | 2D CIR. (fn8) | FFT | DIFF. |
|-----------------|--------------------|---------------------|----------------------------|------------|--------------|
| 0 | 10000 | 10000 | 10000 | 10000 | 10000 |
| 1 | -0.040 | -0.040 | -0.010 | -0.010 | -0.040 |
| 2 | 0.024 | 0.024 | 0.102 | 0.102 | 0.021 |
| 3 | -0.012 | -0.013 | -0.006 | -0.006 | -0.013 |
| 4 | 0.130 | 0.119 | 0.123 | 0.123 | 0.215 |
| 5 | 0.001 | 0.004 | -0.002 | -0.002 | 0.005 |
| 6 | 0.013 | 0.182 | -0.018 | -0.018 | -0.823 |
| 7 | -0.002 | -0.002 | 0.000 | 0.000 | -0.009 |
| 8 | -0.058 | -0.890 | -0.028 | -0.028 | 5.390 |

This coarse case has 2 ppm difference of Nb_2 and Nb_4 in 2D fits and FFT from the case of a fine mesh. The differential field Nb_8 of the coarse case has one part in ten thousand difference from the case of a fine mesh.

The curve of the differential distribution for the OPERA 3D dipole magnet is shown in Fig. 3. The third differential distribution resembles that in OPERA 2D, but the curve begins to oscillate from the fourth differential curve, and deteriorates progressively at each next step.

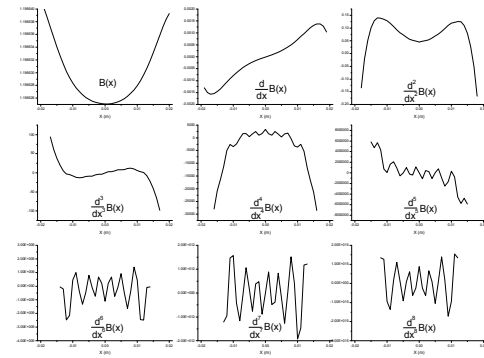


Figure 3: Eighth differential of $B_y(x)$ in OPERA 3D.

CONCLUSION

The results of analytic methods of four kinds for a simulation are presented in this paper. The consistency of these four methods is satisfactory in the OPERA 2D case; the difference is within 1 ppm in the allowed term. The fit number for 1D fits and 2D elliptic fits should be carefully chosen for components of high order. The 2D circular fits and the FFT results of OPERA 3D are similar to those of OPERA 2D; the difference is also only 1 ppm in allowed terms. The 1D fits and the results of the differential method of OPERA 3D have large errors in multipole components of high order.

REFERENCES

- [1] J. C. Jan et al., "Precise Rotating Coil System for Characterizing the TPS Magnets", Proceedings of the PAC'09, June 2009, p. 199 (2009).
- [2] Vector Field Opera, "2D reference manual version 13"